On the synthesis of quantum Hall array resistance standards

On the synthesis of Quantum Hall Array Resistance Standards

Massimo Ortolano[1,3], Marco Abrate[2] and Luca Callegaro[3],

[1] Dipartimento di Elettronica e Telecomunicazioni, Politecnico di Torino
Corso Duca degli Abruzzi 24, 10129 Torino, Italy
[2] Dipartimento di Scienze Matematiche, Politecnico di Torino
Corso Duca degli Abruzzi 24, 10129 Torino, Italy
[3]INRIM - Istituto Nazionale di Ricerca Metrologica
Strada delle Cacce, 91 - 10135 Torino, Italy

Abstract. Quantum Hall effect (QHE) is the basis of modern resistance metrology. In Quantum Hall Array Resistance Standards (QHARS), several individual QHE elements, each one having the same QHE resistance (typically half of the von Klitzing constant), are arranged in networks that realize resistance values close to decadic values (such as 1 kΩ or 100 kΩ), of direct interest for dissemination. The same decadic value can be approximated with different grades of precision, and even for the same approximation several networks of QHE elements can be conceived. The paper investigates the design of QHARS networks by giving methods to find a proper approximation of the resistance of interest, and to design the corresponding network with a small number of elements; results for several decadic case examples are given. The realization of these networks with multiterminal QHE elements requires a new *multiple bridge* connection, here described.

1. Introduction

Quantum Hall Array Resistance Standards (QHARS) [1–11] are integrated circuits in which several quantum Hall elements are interconnected to compose a resistive network. QHARS are of great interest for electrical metrology because they allow the representation of the ohm in the International System of Units. In particular, reliable QHARS having resistance values close to decadic values (e.g., 100 Ω, 1 kΩ, 10 kΩ) would allow the calibration of artifact resistance standards of practical interest by 1:1 ratio bridges, which do not require ratio calibration, or even by substitution.

QHARS require dedicated foundries and the development of novel realization methods, in particular for what concerns wiring and insulation. Although the present integration level allows the realization of QHARS with hundreds of elements, a basic goal of QHARS design is to maximize simplicity, keeping the number of the elements to a minimum.

Recent papers have shown that the same approximation of a decade resistance value R can be realized with networks having a greatly different number of elements; for example, in the realization of a 10 kΩ QHARS, the National Metrology Institute of Japan (NMIJ) evolved from a 266-element network [6] to a 16-element one [11].

The aim of the present paper is to give advice on the synthesis of QHARS networks which approximate a given resistance value within the accuracy required in resistance metrology and employing a minimal number of elements; several cases of practical interest are analyzed and corresponding networks are synthesized. These networks are designed to minimize the effect from contact and wiring resistances and, in addition to the so-called *multiple-series* and *multiple-parallel* connections (see [12] and references therein), they employ a new type of connection, here called the *multiple-bridge*, whose properties are analyzed in section 5.3.

2. The problem

A QHARS is a circuit composed of interconnected elements having the same resistance $R_{\mathrm{H}} = R_{\mathrm{K}}/i$, where R_{K} is the von Klitzing constant and i is the *plateau index* (typically, $i = 2$). The total resistance R of a QHARS is a fraction of the element resistance, $R = (p/q)R_{\mathrm{H}}$, where p and q are positive integers which depend only on the network topology.

The main goal in the design of a QHARS is to obtain a device having a resistance value close to a target value R_0. In the following, for ease of notation, we consider the normalized dimensionless quantities $\rho_0 = R_0/R_{\mathrm{H}}$ (a generic real number) and $\rho = R/R_{\mathrm{H}} = p/q$ (a rational number).

The problem of QHARS network synthesis can be divided into the following steps:

(i) Find a rational approximation $\rho = p/q$ of ρ_0 such that the magnitude of the relative error $\delta = (\rho - \rho_0)/\rho_0$ is less than a specified limit $\delta_{\max}$, that is, $|\delta| < \delta_{\max}$.

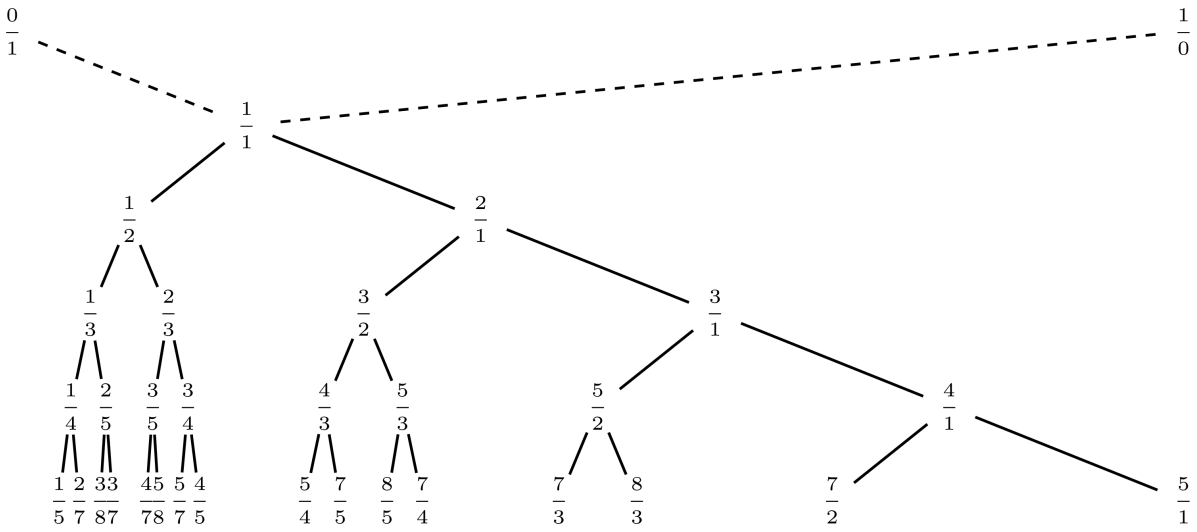

Figure 1. Top levels of the Stern-Brocot tree (for fractions different from 1/0 the horizontal position is to scale).

(ii) Synthesize an optimal network with normalized resistance ρ with a minimal number n of elements.

3. Rational approximations

In this section we consider the problem of obtaining a rational approximation for a given positive real number. Historically, this problem was of particular interest to clockmakers, who had to design accurate gear trains, and led the French clockmaker Achille Brocot to conceive the useful construction which is discussed below‡. The so-called Stern-Brocot tree [14–16] is a binary tree whose nodes are in one-to-one correspondence with the set of positive rational numbers. In particular (figure 1), each node is the mediant fraction $(a + c)/(b + d)$ of the left and right nearest ancestors a/b and c/d (the fractions that can be reached by following the branches upward); the root node is the fraction 1/1, generated from the fictitious ancestors 0/1 and 1/0.

The importance of Stern-Brocot tree in the approximation theory rises up by considering the sequences of rationals, namely the Stern-Brocot sequences, obtained by walking down the nodes of the tree. Given a real number ρ_0, the corresponding Stern-Brocot sequence $\rho_1, \rho_2, \rho_3, \ldots$ can be generated by walking down the tree according to the following rules (see figure 2): start from the tree root $\rho_1 = 1/1$; then, for each $k = 1, 2, 3, \ldots$, if $\rho_0 < \rho_k$, set ρ_{k+1} equal to the left child of ρ_k; otherwise, if $\rho_0 > \rho_k$, set ρ_{k+1} equal to the right child; if, for some k, $\rho_k = \rho_0$, stop (if ρ_0 is rational, the sequence is finite). The Stern-Brocot sequence $\rho_1, \rho_2, \rho_3, \ldots$ obtained in this way converges to ρ_0; moreover, the terms of the sequence are rational approximation of ρ_0 that are optimal in the following sense: if a certain rational approximation of ρ_0 does not belong to the

‡ Before the advent of direct digital frequency synthesizers, time and frequency metrologists —the modern clockmakers— confronted with this problem too (see e.g. [13]).

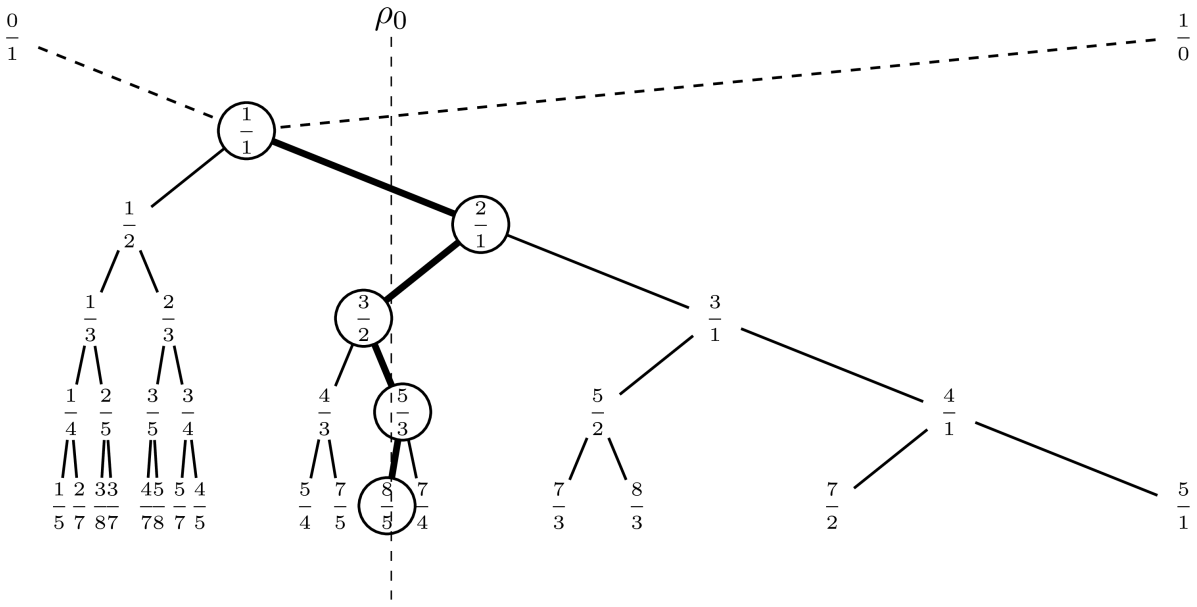

Figure 2. Walking down the Stern-Brocot tree to approximate a real number ρ_0 (here the Stern-Brocot sequence is $\frac{1}{1}, \frac{2}{1}, \frac{3}{2}, \frac{5}{3}, \frac{8}{5}, \ldots$).

sequence, than there is a term of the sequence having smaller numerator or denominator which is a better approximation [16].

A known method to approximate real numbers is that of continued fraction expansion. A continued fraction is a representation of a real number ρ_0 through a sequence of integers as follows:

$$\rho_0 = \alpha_0 + \cfrac{1}{\alpha_1 + \cfrac{1}{\alpha_2 + \cfrac{1}{\alpha_3 + \cdots}}} \,, \tag{1}$$

where the integers $\alpha_0, \alpha_1, \ldots$ are given by the recurrence relations [17]

$$\xi_0 = \rho_0 \,, \tag{2}$$

$$\alpha_k = [\xi_k] \,, \tag{3}$$

$$\xi_{k+1} = \frac{1}{\xi_k - \alpha_k} \,, \quad \text{if } \xi_k \text{ is not an integer,} \tag{4}$$

where $k = 0, 1, 2, \ldots$, and $[\xi_k]$ denotes the integer part of ξ_k. A continued fraction can be expressed in a compact way using the notation $[\alpha_0; \alpha_1, \alpha_2, \alpha_3, \ldots]$.

The finite continued fractions $[\alpha_0; \ldots, \alpha_m]$, for $m = 0, 1, 2, \ldots$, are rational approximations of ρ_0. Given a real number ρ_0, all the rational approximations obtained by continued fraction expansion are included in the Stern-Brocot sequence associated to the same ρ_0. Therefore, approximations obtained by continued fraction expansion need not to be considered separately; moreover, the Stern-Brocot sequence might contain sufficiently accurate approximations to which correspond networks with fewer elements (or other favourable properties) than those of the networks obtained from a

continued fraction expansion (an example is given by the fraction 235/3033 in table 1 of section 4.3).

4. Network synthesis

This section considers the problem of synthesizing a planar resistive network from a given rational approximation $\rho = p/q$ of the target resistance ρ_0. In the following, we consider p and q to be coprimes. Furthermore, since we are dealing with normalized quantities, all elements are of unit value. The systematic generation of such networks was investigated in [18–20].

4.1. Planar networks and square tilings

For a certain ρ, several different equivalent networks having a different number n of elements can be synthesized. A simple example is shown in figure 3, where $\rho = 6/5$ is obtained with two different networks.

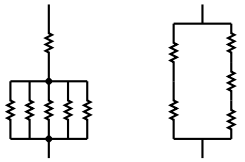

Figure 3. Two different networks with $\rho = 6/5$. The network on the left has $n = 6$ elements, while that on the right has $n = 5$ elements.

A basic network which realizes $\rho = p/q$ in a trivial way is the rectangular network of figure 4, which is composed of $n = pq$ elements arranged in a rectangular grid of height p and width q. For each element, the normalized voltage drop is $1/p$ and the corresponding normalized current is $1/q$.

As shown in figure 4, the rectangular network can be transformed into an equivalent one with fewer elements, by substituting a "square" of $k \times k$ elements with a single element. This new element will sustain a normalized current k/q and a voltage drop k/p will develop on it [21]. Indeed, the normalized power k^2/pq dissipated by this single element is proportional to the area k^2 of the square. The substitution process can be iterated, and any remaining square of elements having side $k > 1$ can be substituted with a single element.

The reader can appreciate that the problem of finding equivalent networks has been related to a geometrical problem: **given a rectangle having integer sides p and q, find a tiling of the rectangle with squares of integer sides** [21–23].

For example, figure 5 shows the two tilings of a 6×5 rectangle corresponding to the two different networks of figure 3; each square of side $k = 1, \ldots, 5$ corresponds a single element, which sustains a voltage $k/5$ and a current $k/6$. Another example is given in figure 6 where two networks which realize the normalized resistance $\rho = 13/11$ are shown with the corresponding tiling superimposed.

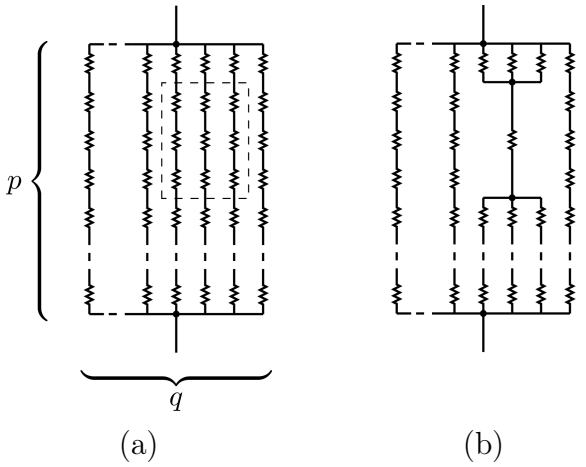

Figure 4. (a) The rectangular $p \times q$ network. (b) A 3×3 square of elements has been substituted with a single element.

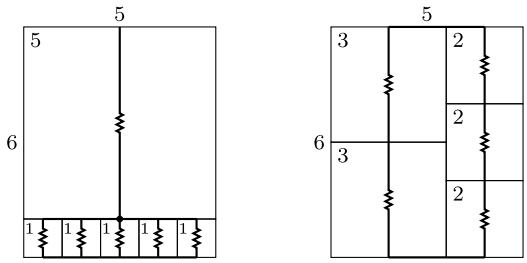

Figure 5. Tilings of the same 6×5 rectangle corresponding to the networks of figure 3.

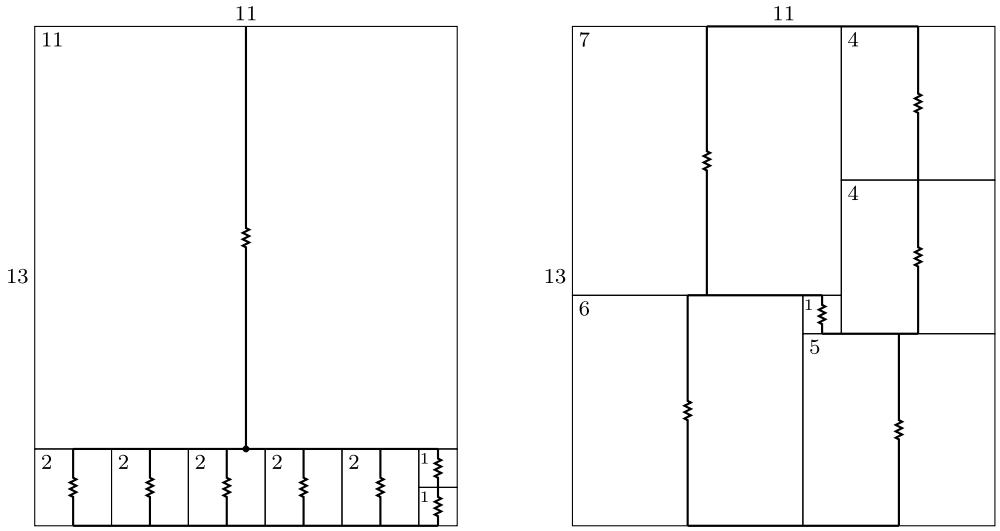

Figure 6. Two different networks with $\rho = 13/11$. The network on the left employs $n = 8$ elements, while the network on the right employs just $n = 6$ elements.

4.2. Minimal tiling

The problem of finding a network with value $\rho = p/q$ having a minimal number of elements is therefore related to the problem of finding a tiling of the rectangle with integer sides p, q having the minimum number $n^*(p, q)$ of integer-sided squares. This problem has been widely studied (see e.g. [21–25]) and the following properties of $n^*(p, q)$ are known [24, 25]:

(i) $n^*(p, q) \geq \max\{p/q, q/p, \log_2 p, \log_2 q\}$;

(ii) $n^*(p, q) \leq \alpha_0 + \alpha_1 + \ldots + \alpha_m \leq \max(p, q)$, where $\alpha_0, \ldots, \alpha_m$ are the elements of the continued fraction expansion of p/q;

(iii) $n^*(p + q, q) = n^*(p, q) + 1$, if $3p \geq q^2$; or, symmetrically, $n^*(p, p + q) = n^*(p, q) + 1$, if $3q \geq p^2$. This property means that for long and thin rectangles for which one of the given conditions is met, the tiling problem can be reduced to that of a smaller rectangle because the tiling includes at least a square with side equal to the shortest side of the original rectangle.

Even though a general solution to the minimal tiling problem is not yet known, there exists an algorithm that performs an exhaustive search§ [25, 27]. To date, all the solutions for $p, q \leq 300$ are known. For larger rectangles, even by taking into account property (iii) to reduce the problem, exhaustive search becomes unfeasible because extremely time-consuming. To overcome this issue, a possibility is that of weakening the condition required in property (iii), so that the original rectangle can be reduced as much as possible before applying exhaustive search, at the cost of accepting possibly non minimal solutions. In this work, where needed, on the basis of [24], the following weakened form of property (iii) is considered‖

(iii′) $n^*(p + q, q) = n^*(p, q) + 1$, if $p \geq q$; or, symmetrically, $n^*(p, p + q) = n^*(p, q) + 1$, if $q \geq p$.

Finally, it is worth noting that, for a network with normalized resistance $\rho = p/q$ and a certain associated tiling, the ratio F between the maximum and the minimum currents in the network is given by the ratio of the side of the largest square of the tiling to that of the smallest square. This follows from the fact noted above that the normalized current which flows through an element corresponding to a square of side k is k/q. The ratio F is an additional figure-of-merit associated to a network [11].

4.3. Cases

In QHARS realized with GaAs technology, the plateau index of interest is $i = 2$, so $R_{\mathrm{H}} = R_{\mathrm{K}}/2$. The recommended value of the the von Klitzing constant is $R_{\mathrm{K}} =$

§ The algorithm recursively fills the target rectangle with squares, in such a way that at each step the filled portion resembles a Young tableau [26]. In this way, the algorithm ensures that each one of the possible tilings is checked only once.

‖ The fact that property (iii′) can lead to non minimal solutions can be demonstrated by considering a 112×53 rectangle for which $n^*(112, 53) = 11 < n^*(59, 53) + 1 = 12$ [25].

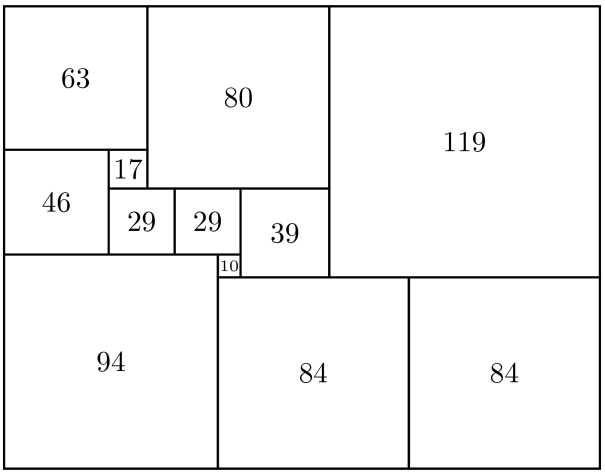

Figure 7. Minimal tiling of the 262-by-203 rectangle.

25 812.807 443 4(84) Ω [3.2×10^{-10}], giving $R_{\mathrm{H}} = R_{\mathrm{K}}/2 = 12\,906.403\,721\,7(42)\,\Omega$ [28]. The conventional value adopted internationally for realizing representations of the ohm is $R_{\text{K-90}} = 25\,812.807\,\Omega_{90}$, giving $R_{\text{H}-90} = R_{\text{K-90}}/2 = 12\,906.4035\,\Omega_{90}$. The relative difference between R_{H} and $R_{\text{H-90}}$ is $1.718(32) \times 10^{-8}$. In the following, the normalization resistance employed to compute ρ_0 and δ is $R_{\text{H-90}}$; however, since approximations ρ to ρ_0 are considered of interest if $|\delta| < 10^{-6}$, the results maintain their validity when R_{H} is instead considered.

We investigate here approximations of decadic resistance values, in particular the values 100 Ω, 1 kΩ, 10 kΩ, 100 kΩ and 1 MΩ. These values are often those for which a set of artifact resistance standards is maintained, are typically calibrated for dissemination, and are the goal of previous works on QHARS design [4, 6–8, 11]. With available QHARS of these values, the dissemination process could proceed mainly by substitution or 1 : 1 comparison calibrations, which do not require the availability of resistance ratio standards that can affect the calibration uncertainty.

Table 1 gives a summary of the results of this investigation. For each decadic value R_0, the normalized ratio $\rho_0 = R_0/R_{\text{K-90}}$ is evaluated. A sequence of rational approximations of ρ_0 is generated from the Stern-Brocot tree. Some cases, selected among those with a maximum error of 10^{-6} or better, are developed¶; one case ($\rho = 203/262$) is taken as example to outline the complete analysis.

The rectangle corresponding to each approximation ρ is tiled by squares, using the method described in section 4. Figure 7 shows the tiling found for the example case 203/262, which corresponds to a minimal tiling (for the other cases, it might occur that further simpler tilings exist). For each case, the number n of QHE network elements involved, the F ratio value and the network topology can be directly deduced from the tiling. Figure 8 shows the network topologies found for several cases of interest.

¶ Some of the approximations were previously investigated in [8, 11], also. Table 1 reports the number of elements in the networks there considered, and the corresponding F ratio.

Table 1. Summary of the cases analyzed in this work: $\rho_0 = R_0/R_\mathrm{H}$ is the normalized target value, $\rho = p/q$ is a rational approximation for ρ_0 and $\delta = (\rho - \rho_0)/\rho_0$ is the relative error of the approximation. For each approximation, the last four columns report the properties of the corresponding solution obtained with the algorithm described in section 4: n is the number of elements composing the network and F is the ratio between the maximum and the minimum currents. For some solutions, the last column gives a reference to the corresponding network topology in figure 8. Where applicable, for comparison, the results from [11] are also reported.

		Results from [11]		This work			
ρ	δ	n	F	n	F	Minimal	Figure
			$R_0 = 100\,\Omega$				
47/6066	$+1.6 \times 10^{-6}$			137	47/4	No	8(a)
78/10067	-5.2×10^{-7}	151	78	138	78	No	8(b)
125/16133	$+2.7 \times 10^{-7}$			139	125/7	No	
203/26200	-3.4×10^{-8}			140	203/10	No	
			$R_0 = 1\,\mathrm{k}\Omega$				
203/2620	-3.4×10^{-8}			24	203/12	No	8(c)
235/3033	$+1.6 \times 10^{-6}$	30	47	24	235/17	No	8(d)
			$R_0 = 10\,\mathrm{k}\Omega$				
203/262	-3.4×10^{-8}	16	67/11	12	119/10	Yes	8(e)
			$R_0 = 100\,\mathrm{k}\Omega$				
1015/131	$+3.4 \times 10^{-8}$	23	131/2	18	131/4	No	8(f)
			$R_0 = 1\,\mathrm{M}\Omega$				
4029/52	$+1.9 \times 10^{-6}$			88	52/2	No	
6121/79	-1.2×10^{-6}			87	79/2	No	8(g)
10150/131	$+3.4 \times 10^{-8}$	98	131	88	131/2	No	8(h)

5. Device connections

This section analyzes the problem of realizing the networks synthesized in section 4 with QHE elements. All the networks shown in figure 8 are represented as two-terminal networks composed of two-terminal elements. Concrete circuits, instead, are provided with four terminals (two current terminals and two voltage ones) and, in order to reject the effect of the inevitable contact and wiring resistances, the interconnections among the elements are realized as multiterminal connections.

5.1. Notation

In what follows, QHE elements are labelled with lower-case letters. The magnetic flux density $\boldsymbol{B}$ is assumed to be pointing out of the page. All QHE elements are supposed to be in the same fully quantized state. The notation given below is partly taken from [12, 29]:

- $r = R_{\mathrm{H}}/2$ is the resistance associated with the Ricketts-Kemeny model [30] of a QHE element;
- $\epsilon_{k\mathrm{x}}\, r$ is the resistance of contact k (including the wiring resistance) of element x;
- $\epsilon = \max\{\epsilon_{k\mathrm{x}}\}$;
- $O(\bullet)$ is the *big O notation*, which represents the order of magnitude of the dependence on $\bullet$.

5.2. Multiple-series and parallel connections

QHARS reported in the literature are based on the repeated application of the so-called *multiple-series* or *multiple-parallel* connections. The denomination of these connections is taken from the usual series or parallel connection of two-terminal resistors. These connections are characterized by an order m [29]. The double-series and double-parallel connections ($m = 2$) are shown in figure 9.

It was shown in [12, 29, 31] that

$$R_{\mathrm{S}}^{(m)} = 2R_{\mathrm{H}}\left(1 + O(\epsilon^m)\right), \qquad R_{\mathrm{P}}^{(m)} = \frac{1}{2}R_{\mathrm{H}}\left(1 + O(\epsilon^m)\right), \tag{5}$$

where $R_{\mathrm{S}}^{(m)}$ and $R_{\mathrm{P}}^{(m)}$ are the four-terminal resistances of the m-series and m-parallel connection of the two QHE elements, respectively.

5.3. Multiple-bridge connection

The two-terminal networks of section 4 not only include series or parallel connections, but also *bridge* connections. Therefore, to realize these networks with QHE elements the multiple-series and -parallel connections are no longer sufficient, and a *multiple-bridge* connection has to be introduced.

For example, figure 10 shows the realization of the network of figure 6 (right) with six QHE elements in double-series, double-parallel and double-bridge connections. The four-terminal resistance $R_{\mathrm{B}}^{(2)}$ of this network, computed with the method described in [12], is

$$\begin{aligned} R_{\mathrm{B}}^{(2)} = \frac{13}{11}R_{\mathrm{H}}\Bigg(1 &+ \frac{49\epsilon_{1\mathrm{a}}\epsilon_{2\mathrm{a}}}{1144} - \frac{7\epsilon_{1\mathrm{a}}\epsilon_{2\mathrm{b}}}{286} - \frac{7\epsilon_{1\mathrm{b}}\epsilon_{2\mathrm{a}}}{286} + \frac{2\epsilon_{1\mathrm{b}}\epsilon_{2\mathrm{b}}}{143} \\ &+ \frac{2\epsilon_{1\mathrm{c}}\epsilon_{2\mathrm{c}}}{143} + \frac{2\epsilon_{1\mathrm{c}}\epsilon_{4\mathrm{b}}}{143} + \frac{\epsilon_{1\mathrm{d}}\epsilon_{2\mathrm{d}}}{858} - \frac{\epsilon_{1\mathrm{d}}\epsilon_{2\mathrm{e}}}{286} \\ &+ \frac{7\epsilon_{1\mathrm{d}}\epsilon_{4\mathrm{a}}}{1716} - \frac{\epsilon_{1\mathrm{e}}\epsilon_{2\mathrm{d}}}{286} + \frac{6\epsilon_{1\mathrm{e}}\epsilon_{2\mathrm{e}}}{143} + \frac{7\epsilon_{1\mathrm{e}}\epsilon_{4\mathrm{a}}}{286} \\ &+ \frac{25\epsilon_{1\mathrm{f}}\epsilon_{2\mathrm{f}}}{858} + \frac{5\epsilon_{1\mathrm{f}}\epsilon_{4\mathrm{c}}}{429} + \frac{5\epsilon_{1\mathrm{f}}\epsilon_{4\mathrm{d}}}{1716} + \frac{2\epsilon_{2\mathrm{c}}\epsilon_{3\mathrm{b}}}{143} \\ &+ \frac{7\epsilon_{2\mathrm{d}}\epsilon_{3\mathrm{a}}}{1716} + \frac{7\epsilon_{2\mathrm{e}}\epsilon_{3\mathrm{a}}}{286} + \frac{5\epsilon_{2\mathrm{f}}\epsilon_{3\mathrm{c}}}{429} + \frac{5\epsilon_{2\mathrm{f}}\epsilon_{3\mathrm{d}}}{1716} \\ &+ \frac{49\epsilon_{3\mathrm{a}}\epsilon_{4\mathrm{a}}}{858} + \frac{2\epsilon_{3\mathrm{b}}\epsilon_{4\mathrm{b}}}{143} + \frac{8\epsilon_{3\mathrm{c}}\epsilon_{4\mathrm{c}}}{429} - \frac{\epsilon_{3\mathrm{c}}\epsilon_{4\mathrm{d}}}{429} \\ &- \frac{\epsilon_{3\mathrm{d}}\epsilon_{4\mathrm{c}}}{429} + \frac{\epsilon_{3\mathrm{d}}\epsilon_{4\mathrm{d}}}{858} + \frac{9\epsilon_{3\mathrm{e}}\epsilon_{4\mathrm{e}}}{286} - \frac{15\epsilon_{3\mathrm{e}}\epsilon_{4\mathrm{f}}}{572} \end{aligned}$$

$$- \frac{15\epsilon_{3f}\epsilon_{4e}}{572} + \frac{25\epsilon_{3f}\epsilon_{4f}}{1144}\Bigg),$$

$$= \frac{13}{11} R_{\mathrm{H}} \left(1 + O(\epsilon^2)\right). \tag{6}$$

Equation (6) shows that the double-bridge connection allows the rejection of the parasitic resistances to the order $O(\epsilon^2)$, characteristic of the double-series and double-parallel connections.

Multiple-bridge connections having order $m > 2$ can also be realized. Figure 11 shows a triple-bridge connection of six-terminal QHE elements, having the same topology of figures 6 (right) and 10. The resulting four-terminal resistance has a convoluted expression, which however can be summarized as $R_{\mathrm{B}}^{(3)} = \frac{13}{11} R_{\mathrm{H}} \left(1 + O(\epsilon^3)\right)$, as expected from triple series or parallel connections.

Actually, multiple-series, parallel and bridge connections share the same construction rule: Connect, according to the required topology, all the QHE elements as though they are two-terminal elements. This gives the circuit for the order $m = 1$. Then, to extend the circuit to the order $m = 2$, connect, for each node, the terminals which are the nearest right neighbours of the ones already connected at order 1. This step can be iterated to obtain the circuit for $m = 3$ and beyond.

5.4. Cases

The networks synthesized in section 4 can be all realized with multiterminal QHE elements by employing the connections described in sections 5.2 and 5.3.

The case 203/262 has been fully developed at the order $m = 2$. The corresponding circuit is given in figure 12; the analysis with the method of [12] yields a normalized four-terminal resistance $\rho = 203/262 + O(\epsilon^2)$, as expected; the function $O(\epsilon^2)$ includes 102 terms, the largest of which is $(2023/37990)\epsilon_{3c}\epsilon_{4c}$. It is worth noting that contact resistances ϵ_{3c} and ϵ_{4c} belong to element c, which is the one corresponding to the largest square of figure 7, that is, to the element dissipating the largest power; this fact can probably be related to a theorem by Cohn [32].

6. Conclusions

We have shown that the synthesis of a QHARS with a given value can be traced back to two mathematical problems, well known and widely developed in literature: i) find a rational approximation of the ratio between the QHARS desired value and the quantized resistance; ii) find an efficient tiling of the rectangle representing the approximation fraction with a small number of squares; the tiling will give the number of QHE elements needed and the way to connect them. The networks can then be realized with multiterminal QHE elements by employing multiple connections. A number of cases, corresponding to decadic QHARS resistance values, are explicitly considered, and the 10 kΩ case is fully developed. The resulting networks have a number of elements significantly less than those given in literature.

The authors welcome collaborations with QHARS manufacturers to analyze further cases of practical interest. To those interested, the authors can provide the Mathematica® notebooks of the full calculations developed in this work.

References

[1] Piquemal F P M, Blanchet J, Gèneves G and André J P 1999 *IEEE Trans. Instr. Meas.* **48** 296–300

[2] Poirier W, Bounouh A, Hayashi H, Fhima H, Piquemal F, Gèneves G and André J P 2002 *J. Appl. Phys.* **92** 2844–2854

[3] Bounouh A, Poirier W, Piquemal F, Gèneves G and André J P 2003 *IEEE Trans. Instr. Meas.* **52** 555–558

[4] Poirier W, Bounouh A, Piquemal F and André J P 2004 *Metrologia* **41** 285

[5] Hein G, Schumacher B and Ahlers F J 2004 Preparation of quantum Hall effect device arrays *2004 Conference on Precision Electromagnetic Measurements Digest* pp 273–274

[6] Oe T, Kaneko N, Urano C, Itatani T, Ishii H and Kiryu S 2008 Development of quantum Hall array resistance standards at NMIJ *Precision Electromagnetic Measurements Digest, 2008. CPEM 2008. Conf. on* pp 20–21

[7] Oe T, Matsuhiro K, Urano C, Fujino H, Ishii H, Itatani T, Sucheta G, Maezawa M, Kiryu S and Kaneko N 2010 Development of 10 kΩ quantum Hall array resistance standards at NMIJ *Precision Electromagnetic Measurements (CPEM), 2010 Conference on* pp 619–620

[8] Oe T, Matsuhiro K, Itatani T, Gorwadkar S, Kiryu S and Kaneko N 2011 *IEEE Trans. Instr. Meas.* **60** 2590–2595

[9] Konemann J, Ahlers F J, Pesel E, Pierz K and Schumacher H 2011 *IEEE Trans. Instr. Meas.* **60** 2512–2516

[10] Woszczyna M, Friedemann M, Dziomba T, Weimann T and Ahlers F J 2011 *Appl. Phys. Lett* **99** 022112 (pages 3)

[11] Oe T, Matsuhiro K, Itatani T, Gorwadkar S, Kiryu S and Kaneko N 2013 *IEEE Trans. Instr. Meas.* **62** 1755–1759

[12] Ortolano M and Callegaro L 2012 *Metrologia* **49** 1

[13] Kroupa V F 1974 *IEEE Tran. Instr. Meas.* **23** 521–524

[14] Stern M A 1858 *Journal für die reine und angewandte Mathematik* **55** 193–220 URL `http://www.digizeitschriften.de/dms/img/?PPN=GDZPPN002150301`

[15] Brocot A 1862 *Calcul des rouages par approximation, nouvelle méthode* (Paris: Achille Brocot) URL `http://gallica.bnf.fr/ark:/12148/bpt6k1661912`

[16] Graham R L, Knuth D E and Patashnik O 1994 *Concrete mathematics* (Addison-Wesley Professional)

[17] Olds C D 1963 *Continued fractions* (New York: Random House)

[18] Amengual A 2000 *Am. J. Phys.* **68** 175–179

[19] Khan S A 2012 *Resonance* **17** 468–475

[20] OEIS Foundation Inc 2013 The on-line encyclopedia of integer sequences sequence A153588 URL `http://oeis.org/A153588`

[21] Cannon J W, Floyd W J and Parry W R 1992 Squaring rectangles: the finite Riemann mapping theorem *The Mathematical Legacy of Wilhelm Magnus: Groups, Geometry, and Special Functions : Proceedings of the Conference on the Legacy of Wilhelm Magnus* ed Abikoff W, Birman J S and Kuiken K (Brooklyn, NY, US: American Mathematical Society)

[22] Brooks R L, Smith C A B, Stone A H and Tutte W T 1940 *Duke Math. J* **7** 312–340

[23] Bouwkamp C J 1946 On the dissection of rectangles into squares (I–III) *Koninklinjke Nederlandsche Akademie van Wetenschappen, Proceedings* vol 49 and 50

[24] Kenyon R 1996 *Journal of Combinatorial Theory, Series A* **76** 272–291

[25] Felgenhauer B 2013 Filling rectangles with integer-sided squares URL `http://int-e.eu/~bf3/squares/`
[26] Yong A 2007 *Notices of the AMS* **54** 270–271
[27] OEIS Foundation Inc 2013 The on-line encyclopedia of integer sequences sequence A219158 URL `http://oeis.org/A219158`
[28] Mohr P J, Taylor B N and Newell D B 2012 *Rev. Mod. Phys.* **84** 1527–1605
[29] Delahaye F 1993 *J. Appl. Phys.* **73** 7914–7920
[30] Ricketts B W and Kemeny P C 1988 *J. Phys. D: Appl. Phys.* **21** 483
[31] Cage M, Jeffery A, Elmquist R and Lee K 1998 *J. Res. NIST* **103** 561–592
[32] Cohn R M 1950 *Proc. Amer. Math. Soc* **1** 316–324

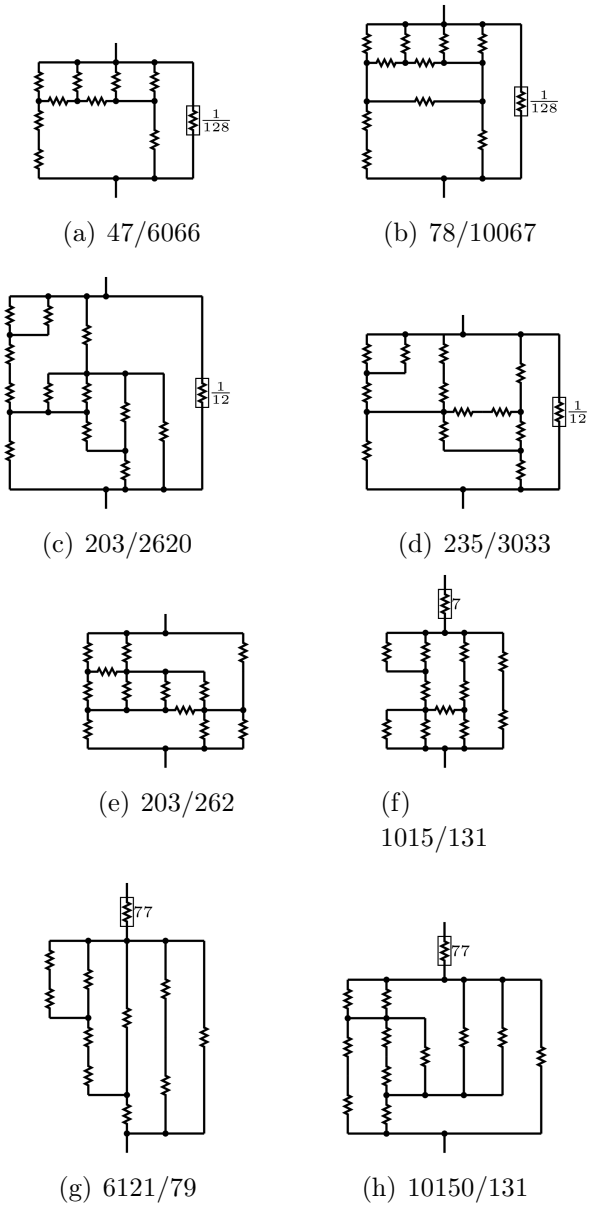

(a) 47/6066 (b) 78/10067

(c) 203/2620 (d) 235/3033

(e) 203/262 (f) 1015/131

(g) 6121/79 (h) 10150/131

Figure 8. Network topologies corresponding to the cases considered in table 1. Boxed resistor symbols labelled as N (or $1/N$) represent a series (or a parallel) of N elements.

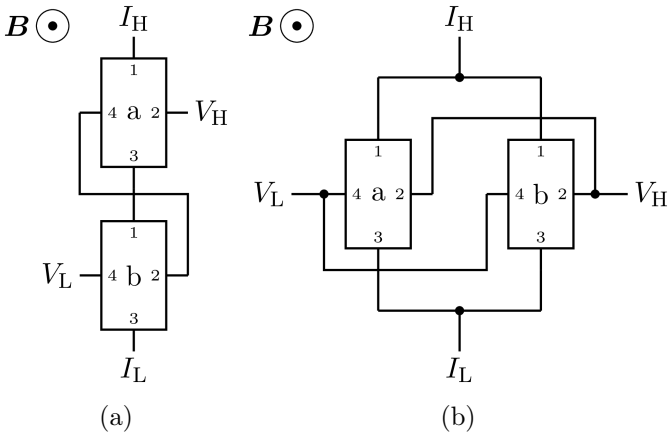

Figure 9. (a) Double series and (b) double parallel connection of two quantum Hall elements. Each element is provided with two current contacts (1,3) and two voltage contacts (2,4). The resulting networks have two current terminals (I_H, I_L) and two voltage terminals (V_H, V_L) each.

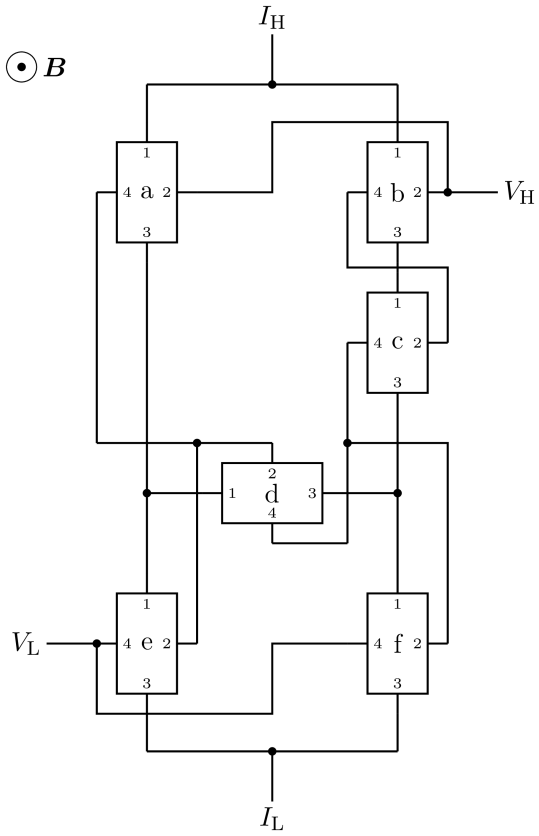

Figure 10. A network of six QHE elements, with a topology corresponding to that of figure 6 (right) and including a double-bridge connection. The elements are provided with two current contacts (1,3) and two voltage contacts (2,4). The network has two current terminals (I_H, I_L) and two voltage terminals (V_H, V_L).

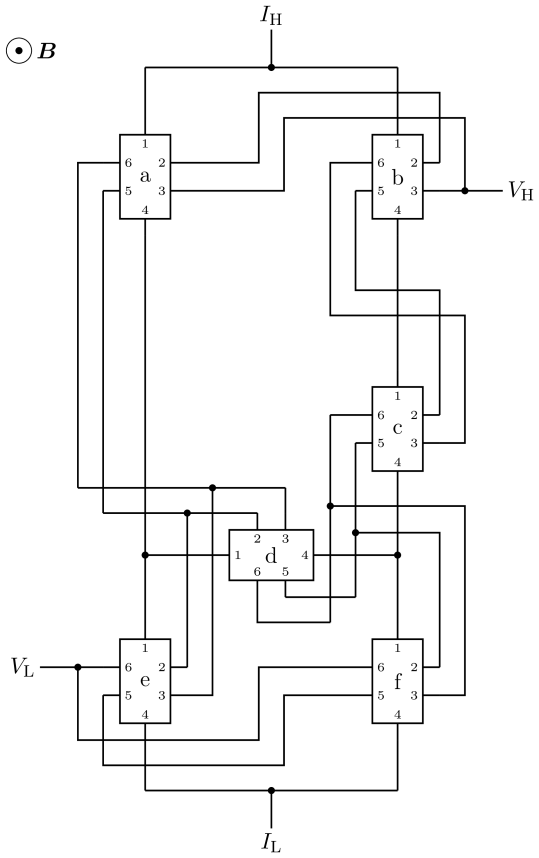

Figure 11. The same network of figure 10, here realized at order $m = 3$. Each element is now provided with two current contacts (1,4) and four voltage contacts (2,3,5,6).

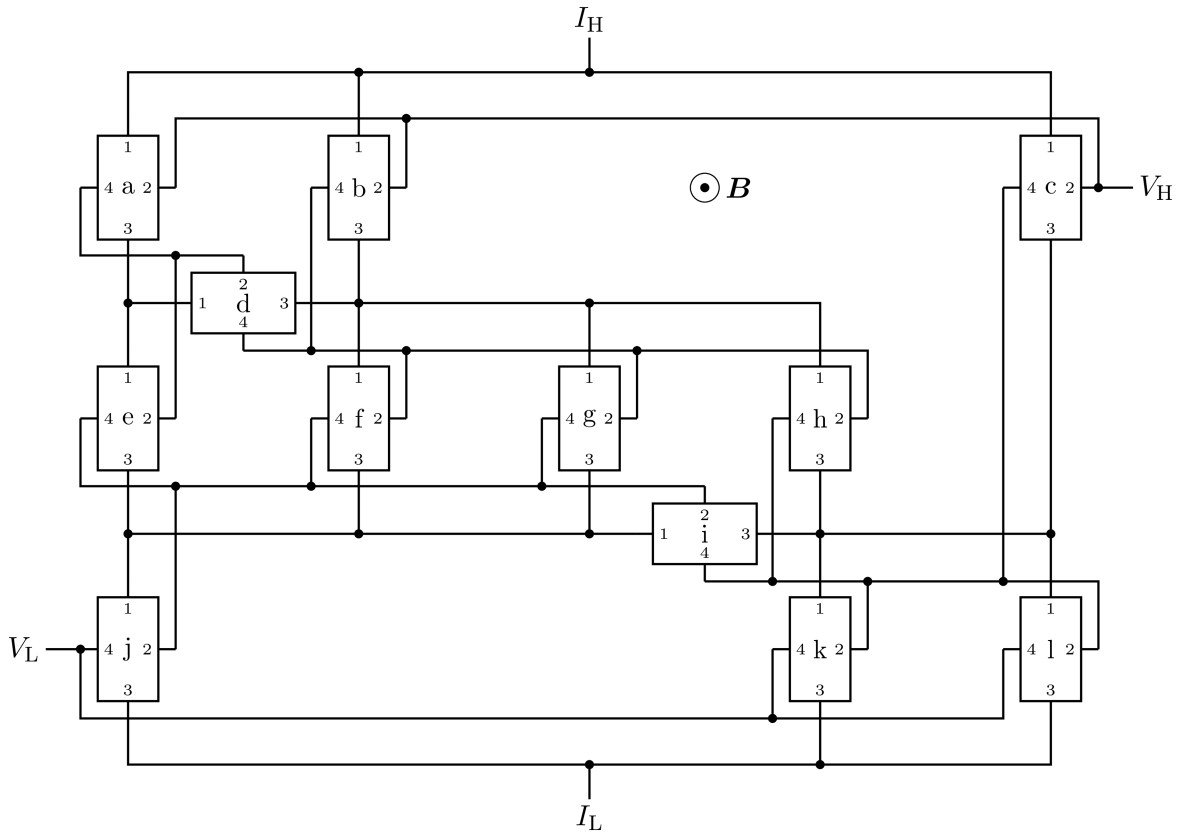

Figure 12. Circuit diagram corresponding to the tiling of figure 7 employing 4-terminal QHE elements in multiple-series, multiple-parallel and multiple-bridge connections.